



Computational study on the interaction of a ring-hydroxylating dioxygenase from *Sphingomonas* CHY-1 with PAHs

Vito Librando^{a,b,*}, Matteo Pappalardo^{a,b}

^a Dipartimento di Scienze Chimiche, Università di Catania, Viale A. Doria 6, 95125, Catania, Italy

^b Research Center for Analysis, Monitoring and Minimization Methods of Environmental Risk, Chemical Science Building, Viale A. Doria 6, 95125, Catania, Italy

ARTICLE INFO

Article history:

Received 16 November 2010

Received in revised form 19 January 2011

Accepted 2 March 2011

Available online 8 March 2011

Keywords:

PAH

Bioremediation

Molecular dynamics

Docking

Phnl

ABSTRACT

The massive computational resources available in the framework of a grid paradigm approach represent an emerging tool in the bioinformatics field. In this paper, we used the above approach in the rapid determination of the interactions between the ring-hydroxylating dioxygenase, comprised six enzymatic subunits, and polycyclic aromatic hydrocarbons (PAHs) in their optimal positions. The results were obtained by simulating enzyme dynamics at 300 K through molecular dynamics calculations. For the first time, the equilibrated structure of the dioxygenase revealed a network of channels throughout the enzyme that were sufficiently large to allow a flow of small ions or molecules from the inner core of the complex to its exterior surface. The ring-hydroxylating dioxygenase was able to interact with some of the studied PAHs. Additionally, not only the number of aromatic rings but also the PAH shape were critical in predicting the ability of the dioxygenase to interact with these types of molecules. Docking calculations shed light on a new possible binding site that is far from the enzymatic one, which is potentially interesting in considering the stability of the enzyme itself.

© 2011 Elsevier Inc. All rights reserved.

1. Introduction

Polycyclic aromatic hydrocarbons (PAHs) are ubiquitous environmental pollutants produced in many anthropogenic activities such as the incomplete combustion of coal, oil, gas, lumber, and trash, as well as activities of the petrochemical industry and oil refineries. Furthermore, ships produce heavy marine pollution from effluents and spills. Overall, they are a severe menace to the environment and human health [1]. PAH carcinogenesis involves metabolic activation by P450 mono-oxygenase enzymes to PAH dihydrodiol intermediates, which are transformed into PAH diol epoxides whose epoxide rings reside in sterically crowded bays or fjords. The PAH diol epoxides can react with DNA to form covalent adducts that may ultimately cause tumours.

While two- or three-ring PAHs are easily degraded, high-molecular-weight ones resist biodegradation and persist in the environment [2]. Although low-molecular-weight PAHs are known to be widely removed by pseudomonads, little information is available on the metabolism of high-molecular-weight PAHs [3]. A variety of methods, ranging from solvent extraction to lipophilic adsorbents, have been employed to eliminate or convert environ-

mental PAHs [4], but they are frequently too expensive, particularly for low PAH concentrations.

A common approach to PAH removal is bioremediation using bacteria or enzymes to degrade them [5]. Nevertheless, current knowledge on enzyme bioremediation is limited. Temperature may inhibit its efficiency in some cases [6], whereas PAH concentration may be the key to degradation [7]. Consequently, many authors have suggested engineering an enzyme for bioremediation [8], and a smart approach to PAH removal will likely involve this technique. There are many types of PAHs, but only a small percentage of them are a concern in the environment; thus, an efficient bioremediation tool is needed to attack only selected PAHs.

Some of the most promising sites for PAH removal are oil refineries. Gawad and co-workers [9] directed their attention to the petroleum industry in the Arabian Gulf. Petroleum hydrocarbon contamination is a serious problem in this area, where a large percentage (>50%) of spilled hydrocarbons contain recalcitrant compounds deposited in sediments, beaches and soils [10]. PAH concentrations ranged from 5 to 102.5 mg/kg [11] for residues containing a high percentage of benz(a)anthracene, chrysene and fluoranthene, while other authors cite finding other high-molecular-weight compounds in this region as shown in Fig. 1 [12–15].

Recently, research on better performing, biodegrading enzymes has led to the discovery of a promising protein [16], a ring-hydroxylating dioxygenase (RHD) from *Sphingomonas* CHY-1 called Phnl with the interesting ability to initiate oxidation in a

* Corresponding author at: Dipartimento di Scienze Chimiche, Università di Catania, Viale A. Doria 6, 95125, Catania, Italy. Tel.: +39 095 7385201; fax: +39 095 330424.

E-mail address: vlibrando@unict.it (V. Librando).

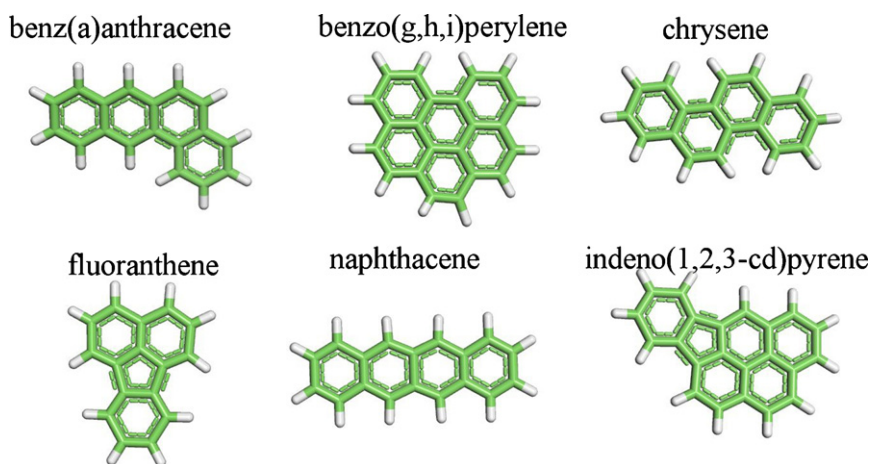


Fig. 1. From top left, benz(a)anthracene, benzo(g,h,i)perylene, chrysene, fluoranthene, naphthalene and indeno(1,2,3-cd)pyrene.

wide range of PAHs. Other studies by the same authors [17] have shed light on this enzyme's ability to degrade some high-molecular-weight PAHs with four and five fused rings. PhnI is an enzyme for bioremediation that still needs optimising, and further engineering should increase its efficiency and selectivity in PAH removal. Work by Jakoncic et al. [16,17] highlighted the potential of this enzyme using very simple docking calculations. In principle, if one is interested in docking studies on a generic enzyme, then only one subset can be adopted as a good model. However, because the contact areas of two domains of a sub-site are considerably hydrophobic, leaving these areas exposed in a docking calculation may lead to unrealistic docking zones. For this reason, we decided to use the entire enzyme in three subsets, each composed of two domains.

The aim of this work was to better characterise PhnI, an enzyme with a Rieske centre domain and a mononuclear iron atom in the active site. Additionally, we studied whether PhnI could degrade PAHs at industrial sites, as previously reported, through a theoretical approach that mixed molecular dynamics and docking calculations [18].

2. Computational details

Molecular dynamics simulation was carried out using NAMD7 [19] software and the CHARMM 22 force field [20]. The simulations started with the experimentally determined X-ray diffraction structures of hydroxylating dioxygenase from *Sphingomonas* sp. CHY-1 (PDB code 2CKF [16]). The structure is composed of three subunits, each one composed of a Rieske-cluster domain and a catalytic domain hosting one mononuclear iron atom. We chose to use all three chains to better characterise the entire protein; simulating only one subunit or domain could lead to artefacts.

The final water box was large enough to contain all of the protein atoms at the end of simulation. The size of the water box was $100 \times 120 \times 110$ Å, with approximately 70,000 water molecules. In all simulation we adopted standard periodic boundary conditions of NAMD, with an all-atoms protein fully solvated in a large box of explicit water, and compute long-range interactions adopting Particle Edwald Mesh method.

The solvated molecules were energy-minimised (conjugate gradient) and gradually heated up to 300 K; they were then equilibrated with a 300 K thermal bath for 400 ps. The timestep was fixed at 2 ps, and the 'rigid bond' NAMD algorithm was used. Non-bond interactions were treated by adopting a cut-off value of 12 Å. All PAH structures utilised in this work were built using a 2D/3D editor from the Accelrys suite and were minimised to a local energy minimum by assigning the CHARMM force field Gasteiger charges [21]

and merging non-polar hydrogen atoms. Sufficiently large grids were chosen to cover significant portions of the enzyme's active pocket [22]. We centred the grid on the mononuclear iron atom of the active site and defined two cubic grids, 40 and 60 Å.

All graphic manipulations and visualisations were performed on the Accelrys suite, whereas ligand docking was performed with Autodock Vina software [23], we adopted standard exhaustivity parameter for the software while its variation do not affects our calculation. The cavity volumes were obtained after iron-atom removal with CAVER software [24]. We adopted the coordinates of the metal ions as the start point for the search path of the cavity. Hence, a spherical probe with a 1.4 Å diameter proceeded from the start point, searching and highlighting all the cavities and paths leading away from the active site of the protein. All calculations were performed on computational resources available by the GRID paradigm managed by "Consorzio COMETA", allowing us to apply computational power of approximately 2000 CPU and 8 Tb RAM.

3. Results

We focused our attention on cavities and the possible pathways connecting the active site with external areas [24]. The coloured surfaces in Fig. 2 represent the principal channels able to conduct a molecule from the outer surface of the protein to the inner core where the mononuclear iron atom is located. Six channels were detected, five of which led outside the protein, while only one, the magenta channel, flowed to the inner core surrounded by the six domains of the protein complex; analysis of such data show that average diameter of channel is 1.6 Å while the smallest diameter correspond to 1.4 Å. This partially explains the experimental data supporting this enzyme as a good PAH degrader.

The first docking step used the larger (60 Å size) grid. A docking calculation was carried out for each of the three mononuclear iron atoms in the active sites. Only chrysene, benz(a)anthracene and naphthalene docked properly – more than 80% of their positions and conformations lay within the active site of the enzyme. Interestingly, the relative positions of the three different molecules lay in very similar positions. Table 1 reports the distance between the mass centre of each residue and the respective mass centre of the docked PAH. This information gives us an idea about docking reproducibility, even if the three molecules are different, and confirms that the method is appropriate for describing the bioremediation properties of the enzyme.

Fig. 3 shows one of the enzyme's active sites with an easily visible iron atom. Each of the three panels clearly shows which PAH points directly at the iron atom. The first PAH degradation step is



Fig. 2. Cartoon representation of PhnI. Coloured surfaces represent cavities as described in the text. Sticked atoms are the three Rieske centres. (For interpretation of the references to colour in this figure legend, the reader is referred to the web version of the article.)

hydrolysis of one covalent bond [25] in the target molecule. Each PAH lies in a similar position, with the short side pointing towards the iron atom and PHE 350, with the side chain of His 207 and Val 208 near the target molecule. HIS 293, THR 308 and LEU 305 define the bottom of the pocket. Being 4 linear, fused benzene rings, the three ligands, chrysene, benz(a)anthracene and naphthalene, share similar spatial occupancies, which offers a possible explanation for their close docking behaviour. In contrast, indeno(1,2,3-cd)pyrene has five fused aromatic rings, and fluoranthene has three fused aromatic rings. They are also expected to interact with this enzyme [17,19], but we did not detect any significant interactions with any of the three active sites. Furthermore, benzo(g,h,i)perylene, with six fused aromatic rings, did not interact with the PhnI active site. Interestingly, the three non-interacting PAHs were found to be well attached to another region of the enzyme, far from any known binding site. We verified that this new binding site was not due to an error in the docking procedure by repeating each calculation and pointing the centre of the grid towards the different mononuclear iron atoms in the active site each time. Each simulation produced similar results, and indeno(1,2,3-cd)pyrene, fluoranthene and benzo(g,h,i)perylene lay in the same region of the protein.

Table 1
Distance between mass centre of each residue with the respective PAH.

	Chrysene	Benz(a)anthracene	Naphthalene
ASN200	8.2	6.1	9.1
PHE201	7.5	8.4	8.0
ASP204	7.9	6.1	8.7
HIS207	6.8	8.8	7.7
VAL208	5.2	7.4	5.7
ILE253	8.7	6.2	8.2
ILE260	6.7	7.6	9.5
HIS293	6.3	9.8	6.0
ASN295	6.8	7.5	6.5
LEU305	8.3	7.5	6.5
THR308	8.4	8.3	7.6
PHE350	7.6	7.6	7.7
LEU356	7.9	7.2	7.4
PHE404	8.4	8.6	8.8

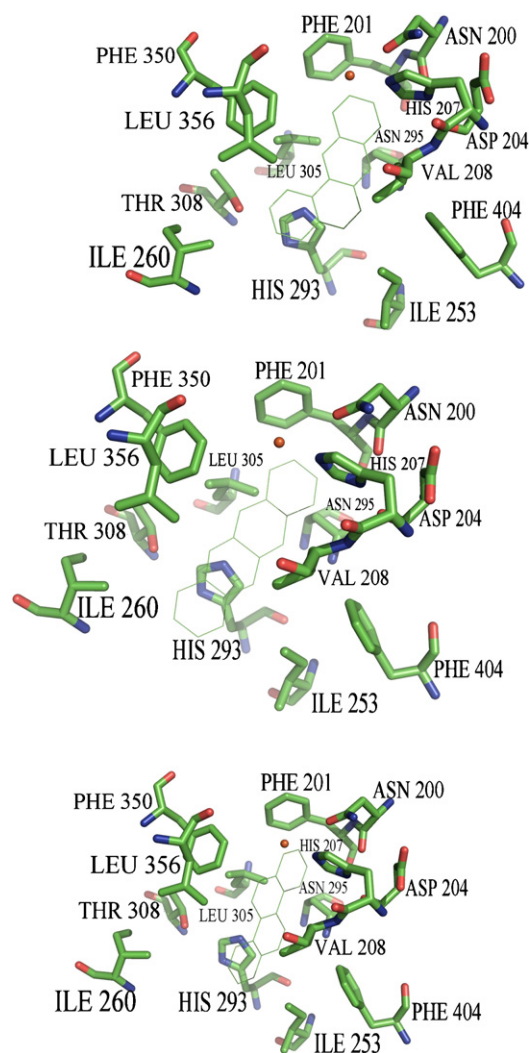


Fig. 3. Docked PAH in the active site cavity of enzyme PhnI. The red sphere represents the mononuclear iron atom. From top to bottom, the docked PAHs are benz(a)anthracene, naphthalene and chrysene. (For interpretation of the references to colour in this figure legend, the reader is referred to the web version of the article.)

Table 2 shows the three PAHs, benzo(g,h,i)perylene, fluoranthene and indeno(1,2,3-cd)pyrene, lying in a protein pocket that was different from any known active sites. All three PAHs share very similar mass centre distances, indicating similar docking positions.

Table 2
Distance between mass centre of each of the three PAH, benzo(g,h,i)perylene, fluoranthene and indeno(1,2,3-cd)pyrene with the mass centre of the aminoacid residue.

	Benzo(g,h,i)perylene	Fluoranthene	Indeno(1,2,3-cd)pyrene
TRP21	10.3	10.4	10.4
TYR57	11.7	11.6	11.5
GLU60	10.7	10.8	10.8
LYS62	10.3	10	9.8
GLN86	10.4	9.9	9.6
HIS89	12.1	11.6	11.4
ARG128	10.4	10.1	10
THR131	6.8	6.9	6.9
GLU132	7.1	7	7
LYS168	10.9	10.6	10.5
ARG317	8.9	9.3	9.4
GLU321	12	12.5	12.6
GLU362	10.3	9.7	9.5
SER366	8.3	7.7	7.5
VAL370	8.9	8.6	8.4

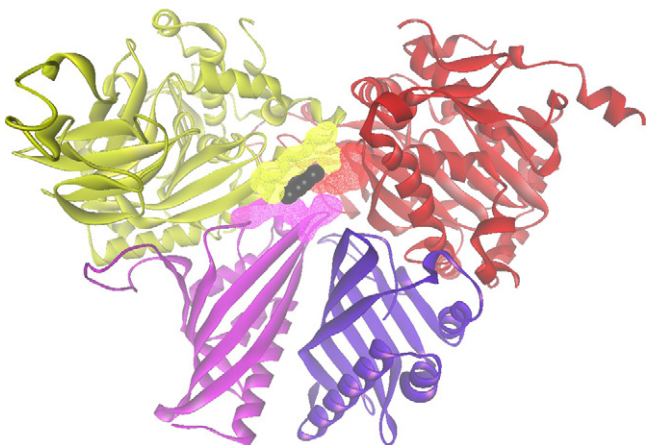


Fig. 4. One of the three PAH (black) docking positions interacting with the secondary docking site of the protein. Each colour represents a single subunit. The docking area is highlighted with the amino acid surface linked to the PAH.

Although the new site does not likely have a direct effect on the biological activity of this enzyme, many hypotheses are possible. In particular, Fig. 4 shows four of six subunits of the protein, each with a different colour. The yellow and red subunits are two of the three degradation domains of this enzyme. The centre of Fig. 3 highlights the black molecule (one of the selected PAH reported in the figure only as an example) interacting with the enzyme and the Van der Waals (WdW) amino acid surfaces in close contact with the ligand. Each amino acid surface has the colour of the parent subunit, and this clearly shows that the PAH is interacting with three different enzyme chains, despite the fact that only biological experiments have confirmed this interaction to date. Altered intra-chain interactions may lead to unwanted molecular damage of the enzyme [26]. Moreover, it is remarkable that this hot spot was detectable only in the complete enzyme, reinforcing our choice to carry out the docking calculations with the entire enzyme complex.

To better understand PAH interactions with this type of enzyme, we decreased the docking area, lessening the grid size to 40 Å. The three molecules, chrysene, benz(a)anthracene and naphthacene, interacted again with the active site of the molecule as expected.

Seventy percent of the selected positions for fluoranthene and indeno(1,2,3-cd)pyrene lay in the active site of the enzyme; their docking calculations were repeated independently for each of the three active protein complexes and resulted in no changes. Table 3 reports the mass centre distances of the PAH ligands with the amino acids of the active site whose values were consistent with the molecules docked in the enzyme. However, comparing the distances for ASN 200, PHE 201, HIS 207, ASN 295 and PHE 350 with the five molecules of interest, it is clear that the last two were greater than the first three. In contrast, the distances for the amino acid PHE 404 were shorter in the last three molecules, with the residual distances remaining mostly constant. The constant distances indicate that these two last PAHs were able to interact with the enzyme, but they lay more shallowly compared to the other molecules. This overview is significant given that PhnI is able to demolish five-ring PAHs; however, we have shown how five-ring ligand molecules are distanced from the mononuclear iron atom compared to the smallest molecules.

Although we are aware that our data cannot be used in biological conclusions, we think that it is useful in furthering drug

Table 4
Mass centre distances (Å) for fluoranthene and indeno (1,2,3-cd)pyrene.

	Fluoranthene	Indeno(1,2,3-cd)pyrene
ASN200	9.1	12,251
PHE201	10.1	11,432
ASP204	11.3	11,322
HIS207	8.7	933
VAL208	5.8	6041
ILE253	7.6	8108
ILE260	8.2	7731
HIS293	5.9	684
ASN295	8.0	9475
LEU305	7.7	894
THR308	7.7	8788
PHE350	8.5	10,331
LEU356	7.5	10,127
PHE404	9.1	914

design and can be used to stimulate further experiments. To highlight this last aspect, Table 4 reports the free binding energies for the PAH molecules with the enzyme for both sets of docking calculations. The data for benz(a)anthracene, chrysene and naphthacene (Table 4) show an almost constant negative binding energy. Benz(a)anthracene, chrysene and naphthacene interacted with the same energies in both search areas (i.e., 40 and 60 Å), indicating that such molecules bind to the same active site in similar manners. In contrast, benzo(g,h,i)perylene, fluoranthene and indeno(1,2,3-cd)pyrene interacted differently energetically in the two aforementioned situations, and the interaction with the active site was approximately 1 kcal mol^{−1}.

Although docking calculations should be the first step in bioremediation experiments, in many cases, its importance is underestimated. We have attempted to initiate bioremediation pathways with two goals: to uphold PAH interactions with the enzyme and engineer a protein that decreases selectivity towards pollutant molecules, thereby increasing the life of such biodegrading systems. Today, most theoretical calculations are only concerned with a small part of the enzyme due to time constraints. By carrying out docking calculations over an entire enzyme containing six protein subunits with more than 28,000 atoms, not counting the water solvent, we found that some of the PAHs used in this work bound selectively to cavities in at least three subunits. Moreover, the protein region binding the pollutant was linked to the active sites of two of the three subunits involved.

While a straightforward biological extrapolation of these results is not simple, the possibility of a secondary docking site existing for such a molecule opens a new scenario in PhnI optimisation. In fact, this region may be a poisoning centre for the enzyme, alter the correct functioning of the active site or, in some cases, may produce misfolding of the enzyme as reported [26]. Furthermore, our calculations provided the opportunity to explore the channel linking the external surface of the protein with the mononuclear iron atom in the active site. The data highlighted at least four of these channels, with one connecting the central area of the enzyme complex. While the external channels were only approximately 1.4 Å diameter, making access difficult for large molecules, the channel connecting the active site with the central channel seemed to be large enough for the transit of large molecules. These large molecules constitute the second part of this work, which is why we studied the interaction of certain strategic PAHs with PhnI. While these results are in agreement the well-known [16] ability of this

Table 3
Binding free energy DG binding (Kcal mol^{−1}) for benz(a)anthracene, benzo(g,h,i)perylene, crysene, fluoranthene, naphthacene, indeno(1,2,3-cd)pyrene.

Grid size (Å)	Benz(a)anthracene	Benzo(g,h,i) perylene	Crysene	Fluoranthene	Naphthacene	Indeno (1,2,3-cd)pyrene
60	−10.3	−9.1	−9.8	−8	−10.1	−8.7
40	−10.2	−7.9	−9.5	−7.4	−9.7	−7.5

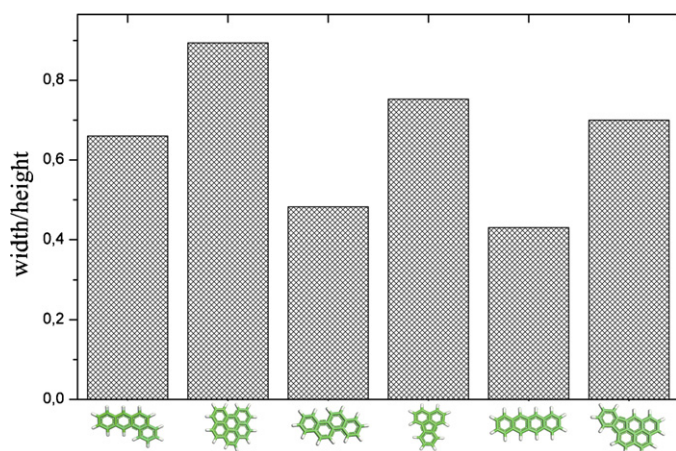


Fig. 5. PAH width/height ratios.

enzyme to degrade large PAHs, they appear more complicated. A three-ring PAH (i.e., fluoranthene) was unable to dock at the active site when we choose large grid, while the four ring PAHs (i.e., benz[a]anthracene, naphthalene and chrysene) interacted preferentially with one of the active sites under the same conditions. There appears to be a width/height ratio threshold (Fig. 5) beyond which molecules have difficulty interacting with the active site. This last concept offers useful information for further experiments of in silico PAH bioremediation through enzyme degradation, with a crucial parameter being not only the number of rings, but, as this work highlights, a low width/height ratio.

4. Conclusions

This work has illustrated the possible role played by PhnI in bioremediation. We found a close network of channels connecting the active site with the outer enzyme complex and demonstrated the importance of carrying out such studies with the entire enzyme complex, not only its functional parts. This approach led us to uncover an interesting docking site that may play an important role in enzyme inhibition. We directed our attention to a series of PAHs known to be present at industrial sites, some of which were not interacted with the PhnI enzyme, demonstrating that while this enzyme complex may be a useful tool for removing such molecules, additional studies are required. Finally, we showed that PAH ring number, together with the width/height ratio, is a good indicator of the binding activities of an enzyme towards PAHs. Further experiments adopting protein assays and cellular tests will be adopted as screening tools for PAH removal using the enzyme of interest.

Acknowledgments

This work has been partially funded by THERMO and MIUR. Computational resources were provided by "Consorzio Cometa".

References

- [1] F.J. Zhang, C. Cortez, R.G. Harvey, New synthetic approaches to polycyclic aromatic hydrocarbons and their carcinogenic oxidized metabolites: derivatives of benzo[s]picene, benzo[rst]pentaphene, and dibenzo[b,def]chrysene, *J. Org. Chem.* 65 (2000) 3952–3960.
- [2] S. Krivobok, S. Kuony, C. Meyer, M. Louwagie, J.C. Willison, Y. Jouanneau, Identification of pyrene-induced proteins in *Mycobacterium* sp strain 6PY1: evidence for two ring-hydroxylating dioxygenases, *J. Bacteriol.* 185 (2003) 3828–3841.
- [3] J.J. Kraus, I.Z. Munir, J.P. McDlood, D.S. Clark, J.S. Dordick, Oxidation of polycyclic aromatic hydrocarbons catalyzed by soybean peroxidase, *Appl. Biochem. Biotechnol.* 80 (1999) 221–230.
- [4] E.C. Santos, R.J.S. Jacques, F.M. Bento, M.D.R. Peralba, P.A. Selbach, E.L.S. Sa, F.A.O. Camargo, Anthracene biodegradation and surface activity by an iron-stimulated *Pseudomonas* sp., *Bioresour. Technol.* 99 (2008) 2644–2649.
- [5] A.K. Haritash, C.P. Kaushik, Biodegradation aspects of polycyclic aromatic hydrocarbons (PAHs): a review, *J. Hazard. Mater.* 169 (2009) 1–15.
- [6] A.M. Farnet, S. Criquet, S. Tagger, G. Gil, J. Le Petit, Purification, partial characterization, and reactivity with aromatic compounds of two laccases from *Marasmius quercophilus* strain 17, *Can. J. Microbiol.* 46 (2000) 189–194.
- [7] G.J. Verrhiest, B. Clement, B. Volat, B. Montuelle, Y. Perrodin, Interactions between a polycyclic aromatic hydrocarbon mixture and the microbial communities in a natural freshwater sediment, *Chemosphere* 46 (2002) 187–196.
- [8] V. Librando, S. Forte, Computer evaluation of protein segments removal effects from naphthalene 1,2-dioxygenase enzyme on polycyclic aromatic hydrocarbons interaction, *Biochem. Eng. J.* 27 (2005) 161–166.
- [9] E.A.A. Gawad, M. Al Azab, M.M. Lotfy, Assessment of organic pollutants in coastal sediments, UAE, *Environ. Geol.* 54 (2008) 1091–1102.
- [10] J.C. Colombo, A. Barreda, C. Bilos, N. Cappelletti, M.C. Migoya, C. Skorupka, Oil spill in the Rio de la Plata estuary, Argentina: 2-hydrocarbon disappearance rates in sediments and soils, *Environ. Pollut.* 134 (2005) 267–276.
- [11] M.D. Fang, C.L. Lee, C.S. Yu, Distribution and source recognition of polycyclic aromatic hydrocarbons in the sediments of Hsin-ta Harbour and adjacent coastal areas, Taiwan, *Mar. Pollut. Bull.* 46 (2003) 941–953.
- [12] A.R. Mostafa, T.L. Wade, S.T. Sweet, A.K.A. Al-Alimi, A.O. Barakat, Distribution and characteristics of polycyclic aromatic hydrocarbons (PAHs) in sediments of Hadhrumout coastal area, Gulf of Aden, Yemen, *J. Mar. Syst.* 78 (2009) 1–8.
- [13] I. Zrafi-Nouira, Z. Khedir-Ghenim, F. Zrafi, R. Bahri, I. Cheraief, M. Rouabhi, D. Saidane-Mosbahi, Hydrocarbon pollution in the sediment from the Jarzouna-Bizerte coastal area of Tunisia (Mediterranean Sea), *Bull. Environ. Contam. Toxicol.* 80 (2008) 566–572.
- [14] Y. Wan, X.H. Jin, J.Y. Hu, F. Jin, Trophic dilution of polycyclic aromatic hydrocarbons (PAHs) in a marine food web from Bohai Bay, North China, *Environ. Sci. Technol.* 41 (2007) 3109–3114.
- [15] V. Fernandez-Gonzalez, S. Muniategui-Lorenzo, P. Lopez-Mahia, D. Prada-Rodriguez, Development of a programmed temperature vaporization-gas chromatography–tandem mass spectrometry method for polycyclic aromatic hydrocarbons analysis in biota samples at ultratrace levels, *J. Chromatogr. A* 1207 (2008) 136–145.
- [16] J. Jakoncic, Y. Jouanneau, C. Meyer, V. Stojanoff, The crystal structure of the ring-hydroxylating dioxygenase from *Sphingomonas* CHY-1, *FEBS J.* 274 (2007) 2470–2481.
- [17] J. Jakoncic, Y. Jouanneau, C. Meyer, V. Stojanoff, The catalytic pocket of the ring-hydroxylating dioxygenase from *Sphingomonas* CHY-1, *Biochem. Biophys. Res. Commun.* 352 (2007) 861–866.
- [18] P.S. Suresh, A. Kumar, R. Kumar, V.P. Singh, An in silico approach to bioremediation: laccase as a case study, *J. Mol. Graph. Model.* 26 (2008) 845–849.
- [19] J.C. Phillips, R. Braun, W. Wang, J. Gumbart, E. Tajkhorshid, E. Villa, C. Chipot, R.D. Skeel, L. Kale, K. Schulten, Scalable molecular dynamics with NAMD, *J. Comput. Chem.* 26 (2005) 1781–1802.
- [20] W.L. Jorgensen, J. Chandrasekhar, J.D. Madura, Comparison of simple potential functions for simulating liquid water, *J. Chem. Phys.* 79 (1983) 926–935.
- [21] J. Gasteiger, M. Marsili, M.G. Hutchings, H. Saller, P. Low, P. Rose, K. Rafeiner, Models for the representation of knowledge about chemical-reactions, *J. Chem. Inform. Comput. Sci.* 30 (1990) 467–476.
- [22] J. Wei, H. Li, W.L. Qu, Q.Z. Gao, Molecular docking study of A(3) adenosine receptor antagonists and pharmacophore-based drug design, *Neurochem. Int.* 55 (2009) 637–642.
- [23] O. Trott, A.J. Olson, Software news and update AutoDock Vina: improving the speed and accuracy of docking with a new scoring function, efficient optimization, and multithreading, *J. Comput. Chem.* 31 (2010) 455–461.
- [24] P. Medek, P. Benes, J. Sochor, Computation of tunnels in protein molecules using Delaunay triangulation, *J. WSCG* 15 (2007) 107–114.
- [25] T. Hadibarata, S. Tachibana, K. Itoh, Biodegradation of chrysene, an aromatic hydrocarbon by *Polyporus* sp S133 in liquid medium, *J. Hazard. Mater.* 164 (2009) 911–917.
- [26] M. Pappalardo, D. Milardi, D. Grasso, C. La Rosa, Steered molecular dynamics studies reveal different unfolding pathways of prions from mammalian and non-mammalian species, *New J. Chem.* 31 (2007) 901–905.